ACS OMEGA

Open Access

http://pubs.acs.org/journal/acsodf

Article

Synthesis of 1-(4-Bromobenzoyl)-1,3-dicyclohexylurea and Its Arylation via Readily Available Palladium Catalyst—Their Electronic, Spectroscopic, and Nonlinear Optical Studies via a Computational Approach

Tahir Maqbool, Humera Younas, Muhammad Bilal, Nasir Rasool,* Majed A. Bajaber, Adeel Mubarik, Bushra Parveen, Gulraiz Ahmad, and Syed Adnan Ali Shah

Cite This: *ACS Omega* 2023, 8, 30306−30314

Read Online

ACCESS | Metrics & More | Article Recommendations | Supporting Information

ABSTRACT: In this study, we reported the synthesis of 1-(4-bromobenzoyl)-1,3-dicyclohexylurea by the reaction of DCC (*N*,*N*′-dicyclohexylcarbodiimide) with 4-bromobenzoic acid. Subsequently, we further synthesized a new series of 1-(4-arylbenzoyl)-1,3-dicyclohexylurea (**5a**−**g**) derivatives using a Suzuki cross-coupling reaction between 1-(4-bromobenzoyl)-1,3-dicyclohexylurea (**3**) and various aryl/heteroaryl boronic acids (**4**). Thus, density functional theory (DFT) calculations have been performed to examine the electronic structure of the synthesized compounds (**3**, **5a**−**g**) and to calculate their spectroscopic data. Moreover, optimized geometries and thermodynamic properties, such as frontier molecular orbitals (HOMO, LUMO), molecular electrostatic potential surfaces, and reactivity descriptors, were also calculated at the PBE0-D3BJ/def2-TZVP/SMD$_{1,4\text{-dioxane}}$ level of theory to validate the structures of the synthesized compounds.

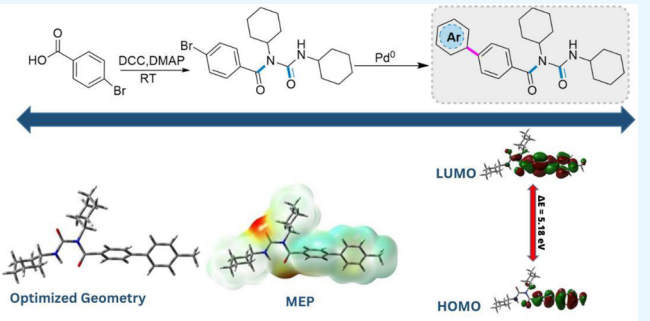

1. INTRODUCTION

The biological activity of *N*-acyl urea, such as anti-inflammatory, anti-helminthic, analgesic, larvicidal, and anti-fungal characteristics, have made them essential.[1] Furthermore, *N*-acyl urea has inhibited the breeding and propagation of domestic flies as well as suppressed the reproduction of the fall armyworm.[2] Since cabergoline acts as a potent prolactin inhibitor, it has been clinically evaluated for treating hyperprolactinemia disorder.[3]

Furthermore, *N*-acyl urea is an essential intermediate in the production of esters and amides.[4] Neves Filho and colleagues proposed using microwaves and solvent-free conditions to synthesize *N*-acyl urea derivatives in 2007. To date, several methods for preparing *N*-acyl urea have been developed. The reaction of DCC with a carboxylic acid in the presence of a base and with or without the usage of DMAP catalyst results in the synthesis of *N*-acyl urea.[5] Soeta et al. described for the first time under aerobic circumstances a catalytic coupling reaction of *N*,*N*′-disubstituted carbodiimides with aldehydes using diverse *N*-heterocyclic carbene precursors.[6] Abbasi and colleagues recently described a green magnetic nanocatalyst reaction of carbodiimides with carboxylic acid to produce *N*-acyl urea.[7]

Compounds containing a biaryl linkage have various applications in pharmaceutical and material sciences.[8] Preparation of novel compounds, when achieved using palladium-catalyzed Suzuki−Miyaura cross-coupling (SMC) of aryl halides with arylboronic acids, is both exceptionally versatile and remarkably expedient since boronic acids are usually nontoxic, chemically inert to air and moisture, and thermally stable and are far easier to handle than other frequently used cross-coupling reagents.[9]

Over the last few years computational chemistry has become an exciting branch for analyzing chemical issues on a laptop or modern computer. It is an associated fast-emerging and exciting discipline that deals with the illustration and also the theoretical calculation of systems like drugs, polymers, biomolecules, organic and inorganic complexes, and molecules. After its advent, it has fully developed to its current state and became standard and vastly benefited from the remarkable enhancements in laptop and computer hardware throughout the last many decennaries. Computational chemistry may be

Received: May 8, 2023
Accepted: July 28, 2023
Published: August 11, 2023

Scheme 1. Formation of 1-(4-Bromobenzoyl)-1,3-dicyclohexylurea (3)[a]

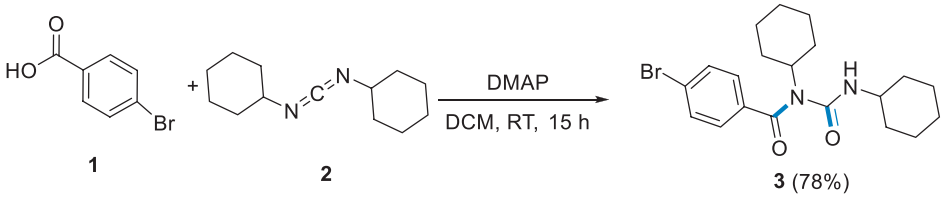

[a]Conditions: (i) **1** (1 g, 4.9 mmol), **2** DCC (1.1 equiv, 5.39 mmol), DMAP (1.5 equiv, 7.35 mmol), and DCM (60 mL), 15 h.

successful in solving complicated biological and chemical issues.[10]

This study focuses on the synthesis of 1-(4-bromobenzoyl)-1,3-dicyclohexylurea (**3**) and its derivatives (**5a−g**) by the SMC reaction. Further, DFT studies are also performed to determine the structural, spectroscopic, and thermodynamic properties such as optimized geometry, frontier molecular orbitals (HOMO−LUMO), molecular electrostatic potential surfaces, electron affinity, ionization energy, chemical softness and hardness, electrophilicity, and chemical potential and the values were compared with each other. The FT-IR and NMR spectra are also performed and compared with the experimental values.

2. RESULTS AND DISCUSSION

2.1. Chemistry. In this study, 1-(4-bromobenzoyl)-1,3-dicyclohexylurea (**3**) was formed by the reaction of 4-bromobenzoic acid (**1**) with DDC (**2**) in the presence of dichloromethane solvent at ambient temperature in a good yield (78%) (Scheme 1).

In the aforementioned reaction, DCC (*N*,*N*′-dicyclohexylcarbodiimide) reacts with 4-bromobenzoic acid (**1**), forming an *O*-acylisourea intermediate. Through an intramolecular rearrangement, the *O*-acylisourea intermediate is transformed into *N*-acyl urea (Scheme 2).[11]

Scheme 2. Intramolecular Rearrangement of *O*-Acylisourea

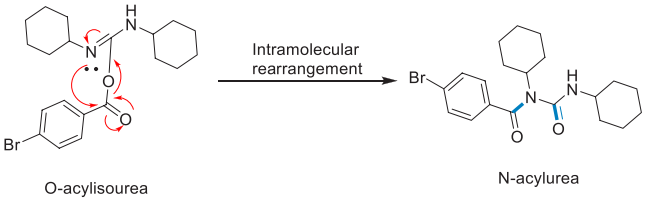

To extend our study, we performed the Suzuki−Miyaura cross-coupling reaction of 1-(4-bromobenzoyl)-1,3-dicyclohexylurea (**3**) with different phenyl boronic acids (**4**), which eventually led to the formation of the corresponding 1-(4-bromobenzoyl)-1,3-dicyclohexylurea (**5a−g**) derivatives in moderate to good yields (30−78%) (Scheme 3). These synthesized derivatives are new to the best of our knowledge. The bulky ligand tetrakis triphenylphosphine attached to the Pd-metal facilitated the heterocoupling between the reacting species rather than undergoing a homocoupling reaction, making the reaction feasible. The solvent used in this coupling reaction is a combination of dioxane and water, as polar solvents can be coordinated with the palladium complex in the transition phase and tend to give better results.[12,13] Since aryl boronic acids with electron-withdrawing moieties are less nucleophilic and therefore transmetalation occurs in a slower manner than that for neutral species as they are more susceptible to undergo side reactions like homocoupling, in the same way, the boronic acids, which are sterically hampered, tend to give lower yields.[13,14]

2.2. Computational Detail. The computational studies of the synthesis compounds (**3**, **5a−g**) were also performed by using the DFT technique to calculate thermodynamic and chemical properties. All the calculations were also performed with a hybrid version of Adamo's Perdew, Burke, and Ernzerhof functional (PBE0)[15] along with the application of Grimme's empirical dispersion correction (D3) with Becke−Johnson damping (D3BJ).[16] The solvent used for all the calculations was 1,4-dioxane induced through the polarizable continuum model (PCM) with the solvent model density (SMD) parameter set by Truhlar.[17] The calculation was performed with Gaussian 09,[18] and all results were visualized using GaussView.[19] The properties such as optimized geometry, frontier molecular orbitals, and HOMO−LUMO energies have been calculated. Global reactivity parameters such as electron affinity, ionization energy, chemical softness and hardness, electrophilicity, and chemical potential have also been calculated.

2.2.1. Optimized Geometries. Geometry optimization is a major component of most computational chemistry studies dealing with the molecules' structure and reactivity. In particular, it relates to geometry optimization methods applied to electronic structure calculations. Because electronic structure calculations can be extensive, geometry optimization methods must be robust and efficient.[20] The three-dimensional optimized geometries of **3** and **5a−g** were calculated at the PBE0-D3BJ/def2-TZVP/$SMD_{1,4\text{-dioxane}}$ level of theory. In 3-dimensional models, the white, yellow, gray, red, green, and light blue colors indicate hydrogen, sulfur, carbon, oxygen chlorine, and fluorine, respectively. The optimized geometries of the compounds under study (**5a−g**) are given in Figure 1.

2.2.2. NMR Spectra. Conformational analysis through NMR spectroscopy is the key to revealing organic compounds. The ^{1}H NMR spectrum provides information about different types of protons and the environment of each of them. Quantum calculations of absolute isotropic magnetic shielding tensors must consider high-quality geometric shapes to produce more reliable results. Numerous studies have focused on the computation of the NMR isotropic magnetic shielding tensor using the gauge-including atomic orbital (GIAO) method in conjunction with density functional theory (DFT).[21] The optimized geometries of all of the compounds were used to calculate the ^{1}H NMR spectra with the PBE0-D3BJ/def2-TZVP/SMD_{DMSO} level of theory using the Gaussian 09 package with the standard GIAO approach to validate the structures of the synthesized compounds. The experimental NMR spectra of compounds **3** and **5a−g** have been given in the Supporting Information (Figures S1−S9). The compar-

https://doi.org/10.1021/acsomega.3c03183
ACS Omega 2023, 8, 30306−30314

Scheme 3. Synthesis of 1-(4-Bromobenzoyl)-1,3-dicyclohexylurea derivatives (5a–g)[a]

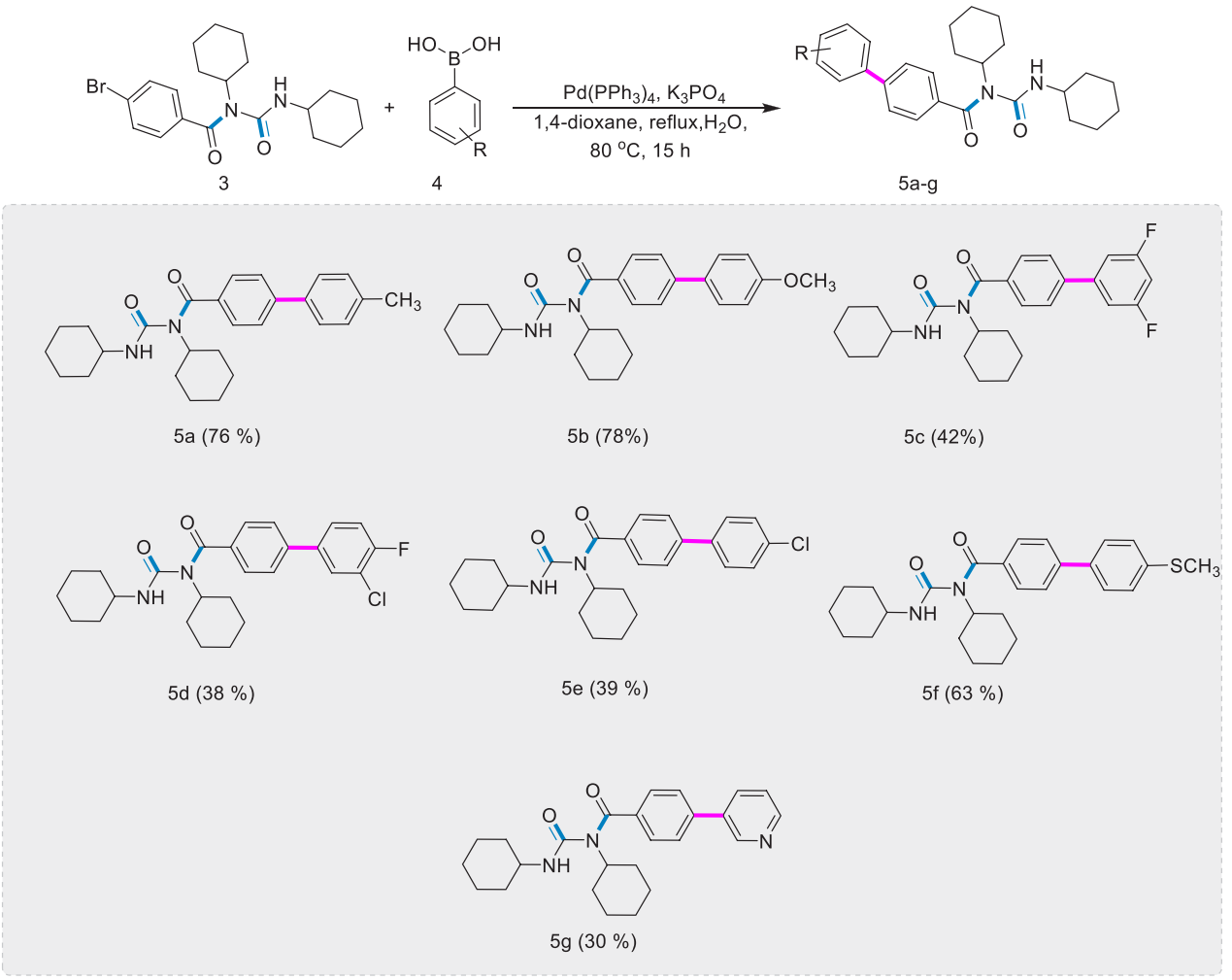

[a]Conditions: (i) **3** (100 mg, 0.28 mmol, 1 equiv), **4** (1.1 equiv), $Pd(PPh_3)_4$ (16 mg, 5 mol %), K_3PO_4 (140 mg, 0.308 mmol, 1.1 equiv), 1,4-dioxane (8 mL), water (0.5 mL), 80 °C, 15 h under argon.

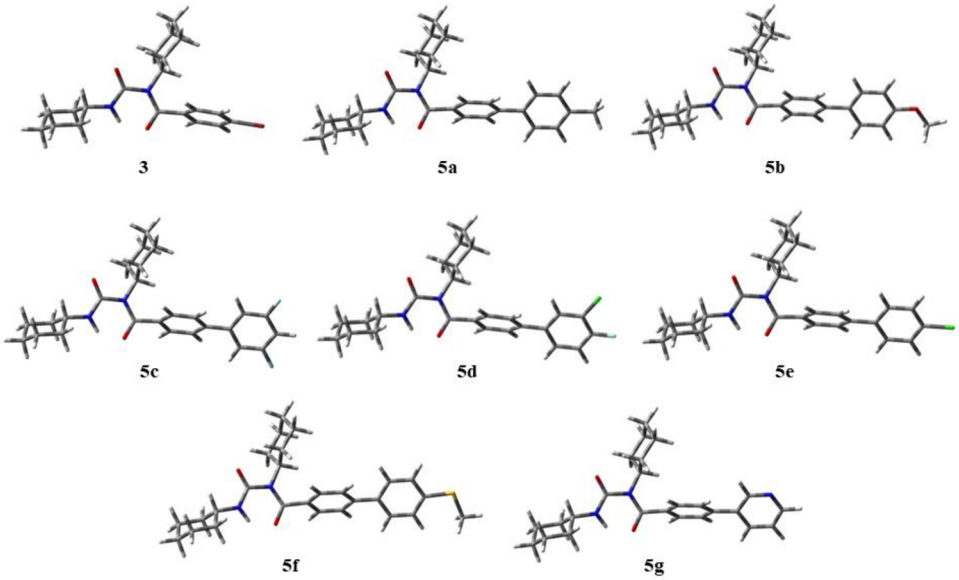

Figure 1. Optimized geometries of all of the synthesized compounds (**3**, **5a–g**) calculated at the PBE0-D3BJ/def2-TZVP/$SMD_{1,4\text{-dioxane}}$ level of theory.

https://doi.org/10.1021/acsomega.3c03183
ACS Omega 2023, 8, 30306–30314

isons of experimental and computed chemical shift values of compound **5a** are given in Table 1; for the rest of the compounds, see the Supporting Information (Tables S1−S7). The experimental and computed values show much resemblance. In the ^{1}H NMR spectrum of compound **5a**, the experimental chemical shift value of all of the aromatic H appears as a doublet in the range 8.00−7.84 ppm, and the computed chemical shift value appears as a doublet in the range 8.01−7.51 ppm.

Table 1. Comparison of Theoretically Calculated and Experimental ^{1}H NMR Data of Compound 5a[a]

Carbon No.	Carbon Type	^{1}H NMR (Experimental) δ, ppm	^{1}H NMR (Computed) δ, ppm	Multiplicity
C_2	CH	8.00	8.01	D
C_3	CH	7.93	7.99	D
C_5	CH	7.93	7.96	D
C_6	CH	8.00	7.82	D
C_8	CH	7.84	7.84	D
C_9	CH	7.75	7.51	D
$C_{10}-CH_3$	CH_3	2.00	2.00	S
C_{11}	CH	7.75	7.51	D
C_{12}	CH	7.84	7.85	D
NH	NH	5.52	5.12	S
N−CH	CH	4.35	4.01	M
NH−CH	CH	3.24	3.12	M
20H Cyclohexyl	CH_2	1.8−0.7	2.60−1.60	M

[a]S = singlet, D = doublet, M = multiplet.

2.2.3. IR Spectra. Infrared spectroscopy is an effective method to identify functional groups in organic molecules. The vibration frequency of compounds **5a−g** was experimentally recorded in the range 4000−600 cm^{-1}. The theoretical IR frequency value of the optimized geometric structure is determined with the basis set of the PBE0-D3BJ/def2-TZVP level of theory. The agreement between the experimental frequency and the theoretical frequency is usually good. The experimental vibration frequency of the 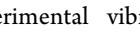 group is observed in the 1696−1623 cm^{-1} range, and the theoretically calculated value lies in the range 1684−1634 cm^{-1}. The groups like 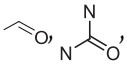 , N−H, etc., are present in all the compounds and are mentioned values in a range. The experimental IR spectra of compounds **3** and **5a−f** are given in the Supporting Information (Figures S10−S16). The selective experimental

Table 2. Selective Experimental and Theoretical Calculated Vibrational Frequencies of Compounds 5a−g with a Scale Factor of 0.89

Groups/Compounds	Experimental Value (cm^{-1})	Calculated Value (cm^{-1})	Assignment
 (In All Compounds)	1696-1623	1684-1634	Stretching
 (In All Compounds)	1644-1622	1771-1634	Stretching
(N-H) (In All Compounds)	3351-3262	3568-3345	Stretching
		1594-1480	Deformation
=C-H (In All Compounds)	2924-2928	3328-3160	Stretching
		1140-1090	Deformation
C-H (In All Compounds)	2853-2849	3214-3050	Stretching
		1481-1354	Deformation
C=C (In All Compounds)	1497-1435	1368-1480	Stretching
CH_3 (**5a, 5b, 5f**)	3160, 3000, 3050	3195, 3265, 3310	Stretching
		902, 1089, 979	Deformation
C-O (**5b**)	1289	1183	Stretching
C-F (**5c, 5d**)	1151, 1185	1249, 1265	Stretching
C-Cl (**5d, 5e**)	828, 821	726, 787	Stretching
C-S (**5f**)	759	705	Stretching
C=N (**5g**)	1537	1520	Stretching

https://doi.org/10.1021/acsomega.3c03183
ACS Omega 2023, 8, 30306−30314

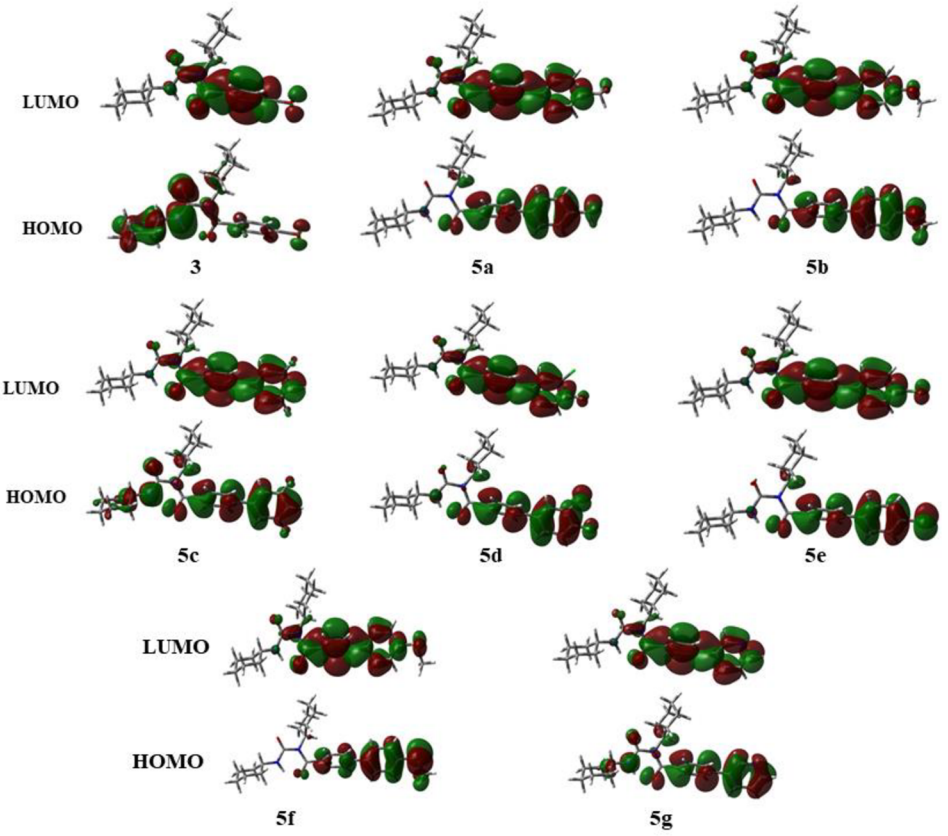

Figure 2. Frontier molecular orbitals of all of the synthesized compounds (**3**, **5a**−**g**) calculated at the PBE0-D3BJ/def2-TZVP/$SMD_{1,4\text{-dioxane}}$ level of theory.

and theoretical calculated vibrational frequencies of compounds **5a**−**g** are given in Table 2.

2.2.4. Frontier Molecular Orbital Analysis and Nonlinear Optics Analysis. The highest occupied molecular orbital (HOMO) and the lowest unoccupied molecular orbital (LUMO) are the most essential orbitals involved in chemical reactions. The HOMO characterizes the ability to donate electrons, and the LUMO characterizes the ability to receive electrons. We can study the reactivity and other different properties of molecules with the help of frontier molecular orbitals (FMOs). The HOMO−LUMO energy difference of the molecule provides us with information about the general reactivity of the molecule. Due to the significant energy difference between the HOMO and the LUMO, the reactivity of the compound becomes more significant, and vice versa.[22] In this series (**5a**−**g**), compound **5c** showed a maximum energy gap of 5.31 eV between the HOMO and the LUMO, which leads to the most stable and least reactive compound in this series, and compound **5f** shows a minimum maximum energy gap of 4.57 eV between the HOMO and the LUMO which led to the most reactive and least stable compound in this series. The frontier molecular orbital maps of all of the synthesized compounds (**3**, **5a**−**g**) are given in Figure 2. The energies of HOMO−LUMO, the HOMO−LUMO gap (ΔE), and hyperpolarizability values are given in Table 3.

The study of nonlinear optical (NLO) substances has interest due to their large number of potential applications, as well as information processing, transmission, and optical data. The molecule has a high hyperpolarizability value and exhibits a high NLO response and vice versa.[23] In this series, compound **5f** consists of 1,3-dicyclohexylurea and biphenyl rings, which further attached the $-SCH_3$ group as a substituent. It shows the highest hyperpolarizability value of 4992.51 Hartree and exhibits a high NLO response as compared to the other compounds because sulfur has a larger size and greater volume occupied by its electrons.

Table 3. Energies of HOMO−LUMO, the HOMO−LUMO Gap (ΔE), and Hyperpolarizability Values

Compounds	E_{HOMO} (eV)	E_{LUMO} (eV)	$\Delta E = E_{LUMO} - E_{HOMO}$ (eV)	Hyperpolarizability (Hartree)
3	−6.96	−1.23	5.73	251.80
5a	−6.47	−1.29	5.18	176.34
5b	−6.12	−1.22	4.90	121.61
5c	−6.89	−1.58	5.31	321.80
5d	−6.74	−1.49	5.25	378.66
5e	−6.63	−1.45	5.18	250.05
5f	−5.91	−1.33	4.58	4992.51
5g	−6.85	−1.50	5.35	200.20

2.2.5. Molecular Electrostatic Potential. The molecular electrostatic potential (MEP) is a 3-dimensional graph showing the charge distribution and charge-related properties of molecules. It gives a graphical understanding of the relative polarity of molecules. MESP can be used to study H-bonding interactions, nucleophilic reactions, and electrophilic attacks. In the MESP maps, the red color shows the electron-rich site related to the electrophilic reactivity. In contrast, blue shows the electron-deficient site related to the nucleophilic reactivity.[24] MESP is a very valuable tool for providing information about molecular interactions. We observed that in

https://doi.org/10.1021/acsomega.3c03183
ACS Omega 2023, 8, 30306−30314

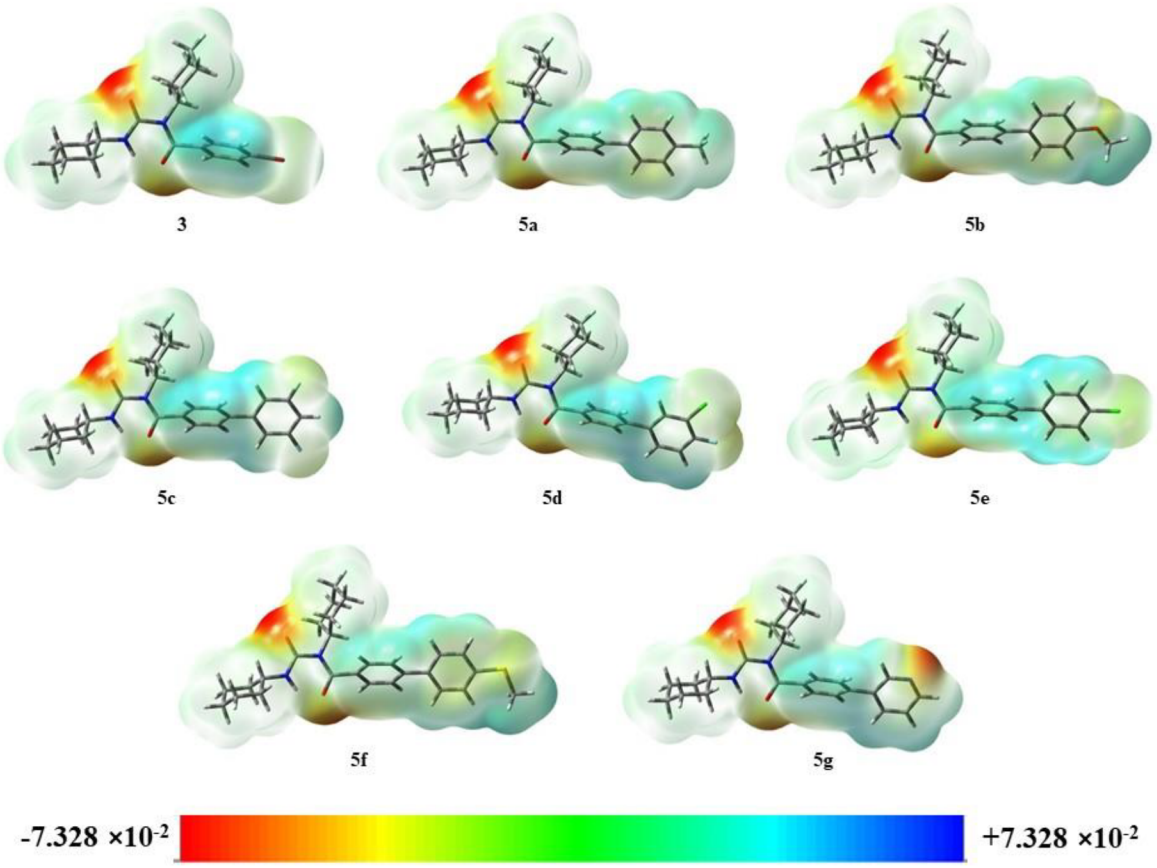

Figure 3. Molecular electrostatic potential maps of all of the synthesized compounds (**3**, **5a**−**g**) were calculated at the PBE0-D3BJ/def2-TZVP/$SMD_{1,4\text{-dioxane}}$ level of theory.

the compounds under study the negative charge is mainly located over the O-atom of urea which is the reactive site for the attack of electrophiles, whereas the positive region is mainly located over the H atoms of the biphenyl group, which is the reactive site for the attack of the nucleophile. The molecular electrostatic potential maps of all of the synthesized compounds (**3**, **5a**−**g**) are given in Figure 3.

2.2.6. Conceptual DFT Reactivity Descriptors. The molecular reactivity and chemical behavior prediction have been carried out through local and global descriptive parameters. The chemical hardness provides the ability to resist changes in the distribution of electrons and is therefore related to the stability and reactivity of molecules, while the chemical flexibility is inversely proportional to hardness. The tendency of molecules to attract electrons is called electronegativity, and its negativeness is called electron chemical potential.[25] Once the chemical system accepts an external charge, the electrophilic index can also be used to measure the energy stability. The ionization potential (I), electron affinity (A), global hardness (η), chemical potential (μ), and electrophilicity index (ω) can be determined from eqs 1, 2, 3, 4, and 5, respectively.[26] The values of reactivity descriptors (I, A, η, μ, and ω) are given in Table 4.

$$I = -E_{\mathrm{HOMO}} \tag{1}$$

$$A = -E_{\mathrm{LUMO}} \tag{2}$$

$$\eta = (I - A)/2 \tag{3}$$

$$\mu = -(I + A)/2 \tag{4}$$

$$\omega = \mu^2/2\eta \tag{5}$$

Table 4. Values of Reactivity Parameters of All of the Synthesized Compounds (3, 5a−g)

Compounds	I (eV)	A (eV)	η (eV)	μ (eV)	ω (eV)
3	6.96	1.23	2.86	−4.09	2.92
5a	6.47	1.29	2.58	−3.88	2.91
5b	6.12	1.22	2.45	−3.67	2.75
5c	6.89	1.58	2.65	−4.23	3.38
5d	6.74	1.49	2.62	−4.11	3.23
5e	6.63	1.45	2.58	−4.04	3.15
5f	5.91	1.33	2.28	−3.62	2.86
5g	6.85	1.50	2.67	−4.179	3.26

3. MATERIALS AND METHODS

3.1. General Information. In the spectroscopic analysis, a 600 MHz Bruker NMR spectrometer and IR were used to validate the synthesized molecules by using deuterated solvents. All of the air- and moisture-sensitive reactions were conducted under an inert atmosphere, particularly in the presence of argon. Moreover, Sigma-Aldrich and Alfa-Aesar provided all of the chemicals that were utilized in this experiment.

https://doi.org/10.1021/acsomega.3c03183
ACS Omega 2023, 8, 30306−30314

3.2. Procedure for the Synthesis of 1-(4-(4-Methylphenyl)benzoyl)-1,3-dicyclohexylurea (3). To a solution of 4-bromobenzoic acid (1 equiv, 4.9 mmol) in DCM and DCC (1.1 equiv, 5.39 mmol) was added DMAP (1.5 equiv, 7.35 mmol). The reaction mixture was allowed to stir under an argon atmosphere for 15 h at room temperature. The reaction progress was monitored by using TLC, methanol, and chloroform (1:9) as solvent systems. After completion of the reaction, a pale yellowish colored product was extracted using DCM. After column chromatography, a good yield of product was retrieved. Elemental analysis, IR, and NMR spectroscopy were used to characterize the desired compound.[27]

3.3. General Procedure for Synthesis of 5a−g. 1-(4-Bromobenzoyl)-1,3-dicyclohexylurea (100 mg, 0.28 mmol, 1.0 equiv), $Pd(PPh_3)_4$ catalyst (16 mg, 5 mol %), and 1,4-dioxane (8 mL) were added in a thoroughly rinsed Schlenk tube. The reaction mixture was degassed using argon. After half an hour of refluxing, boronic acid (1.1 equiv) and K_3PO_4 (1.1 equiv, 0.308 mmol) were added to the above-mentioned mixture. Then, the reaction was allowed to heat for 10 min. Subsequently, 0.5 mL of distilled water was added and refluxed for 15 h at 80 °C. TLC monitored the reaction progress by using *n*-hexane and ethyl acetate (9:1) as a solvent medium. After reaction completion, the product was filtered and purified via column chromatography. The elemental analysis, IR, and NMR techniques were used to investigate the structure of the newly synthesized compounds.[28]

3.4. Characterization Data. *3.4.1. 1-(4-(4-Methylphenyl)benzoyl)-1,3-dicyclohexylurea (**3**).* Pale yellow crystals; M.P. 159−160 °C. ^{1}H NMR (400 MHz, $CDCl_3$) δ: 7.56 (d, J = 8 Hz, 2H), 7.44 (d, J = 8 Hz, 2H), 6.10 (s, 1H), 4.05 (m, 1H) 3.51 (m, 1H), 2.0−0.9 (m, 20H). ^{13}C NMR (100 MHz, $CDCl_3$) δ: 167.3, 156, 136.4, 131.7, 130.1, 125.3, 51.9, 49.5, 33.4, 31.5, 25.9, 24.74, 24.71, 24.69. El. Anal. for $C_{20}H_{27}BrN_2O_2$: Found: C, 58.6; H, 6.5; N, 6.7%. Calculated: C, 58.97; H, 6.68; N, 6.88%.

*3.4.2. 1-(4-(4-Methylphenyl)benzoyl)-1,3-dicyclohexylurea (**5a**).* Yellow crystals; M.P. 130−131 °C. ^{1}H NMR (600 MHz, DMSO) δ: 8.00 (d, J = 6 Hz, 2H), 7.93 (d, J = 6 Hz, 2H), 7.84 (d, J = 6 Hz, 2H), 7.75 (d, J = 6 Hz, 2H), 5.52 (s, 1H), 4.35 (m, 1H) 3.24 (m, 1H), 2.0 (s, 3H) 1.8−0.7 (m, 20H). ^{13}C NMR (100 MHz, $CDCl_3$) δ 167.5, 156.2, 138.9, 138.3, 135.9, 132.1, 130.8, 129.68, 127.28, 126, 52.1, 50.2, 33.5, 32.2, 27.3, 24.94, 24.89, 24.68, 21.34.

*3.4.3. 1-(4-(4-Methoxyphenyl)benzoyl)-1,3-dicyclohexylurea (**5b**).* Yellow crystals; M.P. 143−144 °C. ^{1}H NMR (600 MHz, DMSO) δ: 8.22 (d, J = 9 Hz, 2H), 7.9 (d, J = 9 Hz, 2H), 7.52 (d, J = 9 Hz, 2H), 7.02 (d, J = 9 Hz, 2H), 5.3 (s, 1H), 4.4 (m, 1H), 3.55 (s, 3H), 3.23 (m, 1H), 1.8−0.59 (m, 20H). ^{13}C NMR (100 MHz, $CDCl_3$) δ: 167.8, 156.9, 139.4, 138.7, 136.3, 133, 131.1, 130.5, 128.3, 126.9, 56.4, 52.8, 50.7, 33.9, 32.8, 27.8, 24.96, 24.9, 24.7.

*3.4.4. 1-(4-(3,5-Difluorophenyl)benzoyl)-1,3-dicyclohexylurea (**5c**).* Brown crystals; M.P. 149−150 °C. ^{1}H NMR (600 MHz, DMSO) δ: 8.3 (d, J = 9 Hz, 2H), 7.94 (d, J = 9 Hz, 2H), 7.53 (d, J = 9.6 Hz, 2H), 7.3 (m, 1H), 5.4 (s, 1H), 3.9 (m, 1H) 3.4 (m, 1H), 1.8−0.6 (m, 20H). ^{13}C NMR (100 MHz, $CDCl_3$) δ: 167.3, 164.4, 156, 142.5, 138.4, 131.7, 130.1, 127.8, 109.18, 102.3, 51.9, 49.5, 33.4, 31.5, 25.9, 24.98, 24.9, 24.8.

*3.4.5. 1-(4-(3-Chloro-4-fluorophenyl) benzoyl)-1,3-dicyclohexylurea (**5d**).* Yellow crystals; M.P. 163−164 °C. ^{1}H NMR (600 MHz, DMSO) δ: 7.95 (d, J = 6 Hz, 2H), 7.8 (d, J = 6 Hz, 2H), 7.7 (dd, J_1 = 6 Hz, J_2 = 1.5 Hz, 1H), 7.55 (ddd, J_1 = 8.4 Hz, J_2 = 4.8 Hz, J_3 = 2.6 Hz, 1H), 7.2 (t, 1H), 6.51 (s, 1H), 5.52 (m, 1H), 3.55 (m, 1H), 1.9−0.57 (m, 20H). ^{13}C NMR (100 MHz, $CDCl_3$) δ: 167.42, 156.2, 155.8, 138.4, 136.4, 131.7, 131.4, 130.1, 127.5, 125.3, 124.4, 115.6, 51.9, 49.5, 33.4, 31.5, 25.9, 24.74, 24.71, 24.68.

*3.4.6. 1-(4-(4-Chlorophenyl)benzoyl)-1,3-dicyclohexylurea (**5e**).* Yellow crystals; M.P. 157−158 °C. ^{1}H NMR (600 MHz, DMSO) δ: 7.88 (d, J = 9 Hz, 2H), 7.72 (d, J = 9 Hz, 2H), 7.5 (d, J = 9 Hz, 2H), 7.41 (d, J = 9 Hz, 2H), 4.3 (s, 1H), 3.2 (m, 1H), 2.6 (m, 1H), 1.8−0.55 (m, 20H). ^{13}C NMR (100 MHz, $CDCl_3$) δ: 167.4, 156.2, 138.9, 138.5, 135.3, 132.4, 130.7, 129.7, 127.3, 126, 52.1, 50.4, 33.7, 32.3, 27.5, 24.9, 24.87, 24.7.

*3.4.7. 1-(4-(4-Methylthiophenyl)benzoyl)-1,3-dicyclohexylurea (**5f**).* Yellow crystals; M.P. 139−140 °C. ^{1}H NMR (600 MHz, DMSO) δ: 7.75 (d, J = 9 Hz, 2H), 7.6 (d, J = 9 Hz, 2H), 7.2 (d, J = 9 Hz, 2H), 7.15 (d, J = 6 Hz, 2H), 5.5 (s, 1H), 4.35 (m, 1H, m) 3.34 (m, 1H), 2.5 (s, 3H) 1.9−0.55 (m, 20H). ^{13}C NMR (100 MHz, $CDCl_3$) δ: 167.8, 156.9, 139.4, 138.7, 136.3, 133, 131.1, 130.5, 128.3, 126.9, 52.8, 50.7, 33.9, 32.8, 27.8, 24.96, 24.9, 24.7, 17.8.

*3.4.8. 1,3-Dicyclohexyl-1-(4-(pyridin-3-yl)benzoyl)urea (**5g**).* Green crystals; M.P. 119−120 °C. ^{1}H NMR (600 MHz, DMSO) δ: 8.87 (d, J = 6 Hz, 1H), 8.6 (dd, J_1 = 9 Hz, J_2 = 1.8 Hz, 1H), 8.05 (d, J = 6 Hz, 1H), 7.95 (dd, J_1 = 6.6 Hz, J_2 = 1.5 Hz, 1H), 7.75 (d, J = 6 Hz, 2H), 7.6 (t, 1H), 5.54 (s, 1H), 4.5 (m, 1H) 3.5 (m, 1H), 1.9−0.55 (m, 20H). ^{13}C NMR (100 MHz, $CDCl_3$) δ: 167.5, 156.3, 148.9, 147.8, 137.5, 136.2, 132.9, 130.5, 126, 124.4, 52, 49.8, 33.6, 31.5, 25.9, 24.82, 24.79, 24.7.

4. CONCLUSION

We synthesized 1-(4-bromobenzoyl)-1,3-dicyclohexylurea (**3**) by reaction with DCC and 4-bromobenzoic acid, followed by the synthesis of the arylated acyl urea derivatives (**5a−g**) by SMC. Experimental spectroscopic techniques (NMR, IR) and DFT studies have confirmed the compounds' structure. Further, computational studies have been performed to calculate the thermodynamic and chemical properties, including HOMO and LUMO energy differences. Energies are compared to the entire compound, and the most and least reactive compounds in the series (**5a−g**) are found. The molecular electrostatic potential maps find the active site for the attack of nucleophiles and electrophiles. Compound **5f** shows good NLO properties in the whole series due to the presence of the sulfide group and the substituted cyclohexyl rings, responsible for the poor NLO response for the rest of the molecules. Integrating experimental and computational approaches provides a comprehensive understanding of the compounds' synthesis, structure, reactivity, and properties, enhancing their potential utility across diverse domains.

■ ASSOCIATED CONTENT

Supporting Information

The Supporting Information is available free of charge at https://pubs.acs.org/doi/10.1021/acsomega.3c03183.

Comparison of experimental and computed chemical shift values of NMR (Tables S1−S7); experimental NMR spectra (Figures S1−S9); and experimental IR (Figures S10−S17) (PDF)

https://doi.org/10.1021/acsomega.3c03183
ACS Omega 2023, 8, 30306−30314

AUTHOR INFORMATION

Corresponding Author

Nasir Rasool − *Department of Chemistry, Government College University Faisalabad, Faisalabad 38000, Pakistan*; Email: nasirrasool@gcuf.edu.pk

Authors

Tahir Maqbool − *Department of Chemistry, Government College University Faisalabad, Faisalabad 38000, Pakistan*

Humera Younas − *Department of Chemistry, Government College University Faisalabad, Faisalabad 38000, Pakistan*

Muhammad Bilal − *School of Chemistry and Chemical Engineering, Shandong University, Jinan 250100, China*

Majed A. Bajaber − *Department of Chemistry, Faculty of Science, King Khalid University, Abha 61413, Saudi Arabia*

Adeel Mubarik − *Department of Chemistry, Government College University Faisalabad, Faisalabad 38000, Pakistan*

Bushra Parveen − *Department of Chemistry, Government College University Faisalabad, Faisalabad 38000, Pakistan*

Gulraiz Ahmad − *Department of Chemistry, Government College University Faisalabad, Faisalabad 38000, Pakistan*

Syed Adnan Ali Shah − *Faculty of Pharmacy, Universiti Teknologi MARA Cawangan Selangor Kampus Puncak Alam, 42300 Bandar Puncak Alam, Selangor, Malaysia; Atta-ur-Rahman Institute for Natural Product Discovery (AuRIns), Universiti Teknologi MARA Ca-wangan Selangor Kampus Puncak Alam, 42300 Bandar Puncak Alam, Selangor, Malaysia*

Complete contact information is available at: https://pubs.acs.org/10.1021/acsomega.3c03183

Notes

The authors declare no competing financial interest.

ACKNOWLEDGMENTS

The authors express appreciation to the Deanship of Scientific Research at King Khalid University Saudi Arabia for funding through the research group program under grant number R.G.P. 2/428/44.

REFERENCES

(1) Ranise, A.; Schenone, S.; Bruno, O.; Bondavalli, F.; Filippelli, W.; Falcone, G.; Rivaldi, B. N-Acyl-N-phenyl ureas of piperidine and substituted piperidines endowed with anti-inflammatory and anti-proliferative activities. *Il Farmaco* **2001**, *56* (9), 647−657. Arbuzov, B.; Fedotova, N.; Zobova, N.; Nazyrova, A.; Anan'ev, E.; Gorbunov, S. Synthesis, Antiinflammatory, and Analgesic Activity of N-Acylureas. *Pharm. Chem. J.* **1989**, *23*, 479−481. Karmouta, M. G.; Miocque, M.; Derdour, A.; Gayral, P.; Lafont, O. Synthèse de cyanacétylurées en vue d'essais vis-à-vis d'Hymenolepis nana. *European journal of medicinal chemistry* **1989**, *24* (5), 547−549. Nakagawa, Y.; Akagi, T.; Iwamura, H.; Fujita, T. Quantitative structure-activity studies of benzoylphenylurea larvicides: VI. Comparison of substituent effects among activities against different insect species. *Pestic. Biochem. Physiol.* **1989**, *33* (2), 144−157.

(2) DeMilo, A. B.; Ostromecky, D. M.; Chang, S. C.; Redfern, R. E.; Fye, R. L. Heterocyclic analogs of diflubenzuron as growth and reproduction inhibitors of the fall armyworm and house fly. *J. Agric. Food Chem.* **1978**, *26* (1), 164−166.

(3) Brambilla, E.; Disalle, E.; Briatico, G.; Mantegani, S.; Temperilli, A. Synthesis and nidation inhibitory activity of a new class of ergoline derivatives. *European journal of medicinal chemistry* **1989**, *24* (4), 421−426.

(4) Kishikawa, K.; Eida, H.; Kohmoto, S.; Yamamoto, M.; Yamada, K. Chemoselective alcoholysis of acylureas. *Synthesis (Stuttgart)* **1994**, *1994* (2), 173−175.

(5) Neves Filho, R. A.; Oliveira, R. N. d.; Srivastava, R. M. Microwave-mediated and customery synthesis of N-benzoyl-or N-substituted benzoyl-N, N′-dialkylureas from arylcarboxylic acids and N, N′-disubstituted carbodiimides under solvent-free conditions. *J. Braz. Chem. Soc.* **2007**, *18*, 1410−1414.

(6) Soeta, T.; Tabatake, Y.; Fujinami, S.; Ukaji, Y. N-heterocyclic carbene catalyzed oxidative coupling of aldehydes with carbodiimides under aerobic conditions: Efficient synthesis of N-acylureas. *Org. Lett.* **2013**, *15* (9), 2088−2091.

(7) Abbasi, S.; Miraki, M. K.; Radfar, I.; Karimi, M.; Heydari, A. Efficient Synthesis of N-Acylureas Using Copper Oxide Supported on Magnetic Nanoparticles in Deep Eutectic Solvent. *ChemistrySelect* **2018**, *3* (1), 77−80.

(8) Simonetti, M.; Cannas, D. M.; Larrosa, I. Biaryl synthesis via C−H bond activation: strategies and methods. *Adv. Organomet. Chem.* **2017**, *67*, 299−399.

(9) Miyaura, N.; Suzuki, A. Palladium-Catalyzed Cross-Coupling Reactions of Organoboron Compounds. *Chem. Rev.* **1995**, *95*, 2457.

(10) Jensen, F. *Introduction to computational chemistry*; John Wiley & Sons: 2017. Lewars, E. *Computational chemistry: Introduction to the theory and applications of molecular and quantum mechanics*; Springer: 2011; p 318.

(11) Tsakos, M.; Schaffert, E. S.; Clement, L. L.; Villadsen, N. L.; Poulsen, T. B. Ester coupling reactions−an enduring challenge in the chemical synthesis of bioactive natural products. *Natural product reports* **2015**, *32* (4), 605−632.

(12) Proutiere, F.; Schoenebeck, F. Solvent effect on palladium-catalyzed cross-coupling reactions and implications on the active catalytic species. *Angew. Chem., Int. Ed.* **2011**, *50* (35), 8192−8195. Dawood, K. M.; Fayed, M. S.; Elkhalea, M. M. Heck and Suzuki cross-couplings of aryl and heteroaryl bromides in water using a new palladium (II)-complex. *ARKIVOC* **2010**, *2009*, 324. Liu, C.; Zhang, Y.; Liu, N.; Qiu, J. A simple and efficient approach for the palladium-catalyzed ligand-free Suzuki reaction in water. *Green Chem.* **2012**, *14* (11), 2999−3003.

(13) Chen, Q.; Jiang, P.; Guo, M.; Yang, J. Synthesis of new 2-arylbenzo [b] furan derivatives via palladium-catalyzed Suzuki cross-coupling reactions in aqueous media. *Molecules* **2018**, *23* (10), 2450.

(14) Imran, H. M.; Rasool, N.; Kanwal, I.; Hashmi, M. A.; Altaf, A. A.; Ahmed, G.; Malik, A.; Kausar, S.; Khan, S. U.-D.; Ahmad, A. Synthesis of halogenated [1, 1′-biphenyl]-4-yl benzoate and [1, 1′: 3′, 1 ″-terphenyl]-4′-yl benzoate by palladium catalyzed cascade C−C coupling and structural analysis through computational approach. *J. Mol. Struct.* **2020**, *1222*, 128839. Ahmad, G.; Rasool, N.; Qamar, M. U.; Alam, M. M.; Kosar, N.; Mahmood, T.; Imran, M. Facile synthesis of 4-aryl-N-(5-methyl-1H-pyrazol-3-yl) benzamides via Suzuki Miyaura reaction: antibacterial activity against clinically isolated NDM-1-positive bacteria and their Docking Studies. *Arab. J. Chem.* **2021**, *14*, 103270. Malik, A.; Rasool, N.; Kanwal, I.; Hashmi, M. A.; Zahoor, A. F.; Ahmad, G.; Altaf, A. A.; Shah, S. A. A.; Sultan, S.; Zakaria, Z. A. Suzuki−Miyaura Reactions of (4-bromophenyl)-4, 6-dichloropyrimidine through Commercially Available Palladium Catalyst: Synthesis, Optimization and Their Structural Aspects Identification through Computational Studies. *Processes* **2020**, *8* (11), 1342.

(15) Sellam, A.; Koumina, A.; Bakak, A.; Hadaoui, A.; Heyd, R. Ab Initio Study of the Electronic and Energy Properties of Diamond Carbon. *Applications and Use of Diamond*; IntechOpen: 2023..

(16) Janesko, B. G. Projected Hybrid Density Functionals: Method and Application to Core Electron Ionization. *J. Chem. Theory Comput.* **2023**, *19* (3), 837−847.

(17) Albo Hay Allah, M. A.; Balakit, A. A.; Salman, H. I.; Abdulridha, A. A.; Sert, Y. New heterocyclic compound as carbon steel corrosion inhibitor in 1 M H2SO4, high efficiency at low concentration: experimental and theoretical studies. *J. Adhes. Sci. Technol.* **2023**, *37*, 525.

(18) Frisch, M.; Trucks, G.; Schlegel, H.; Scuseria, G.; Robb, M.; Cheeseman, J.; Scalmani, G.; Barone, V.; Mennucci, B.; Petersson, G. *Gaussian 09*, revision D.01; Gaussian, Inc.: Wallingford, CT, 2009; Vol. *106*.
(19) Dennington, R.; Keith, T. A.; Millam, J. M. *GaussView 6.0.16*; Semichem, Inc.: Shawnee Mission, KS, 2016.
(20) Denzel, A.; Kästner, J. Gaussian process regression for geometry optimization. *J. Chem. Phys.* **2018**, *148* (9), 094114.
(21) Pierens, G. K. 1H and 13C NMR scaling factors for the calculation of chemical shifts in commonly used solvents using density functional theory. *J. Comput. Chem.* **2014**, *35* (18), 1388−1394. Dege, N.; Gökce, H.; Doğan, O. E.; Alpaslan, G.; Ağar, T.; Muthu, S.; Sert, Y. Quantum computational, spectroscopic investigations on N-(2-((2-chloro-4, 5-dicyanophenyl) amino) ethyl)-4-methylbenzenesulfonamide by DFT/TD-DFT with different solvents, molecular docking and drug-likeness researches. *Colloids Surf., A* **2022**, *638*, 128311. Abdulridha, A. A.; Allah, M. A. A. H.; Makki, S. Q.; Sert, Y.; Salman, H. E.; Balakit, A. A. Corrosion inhibition of carbon steel in 1 M H2SO4 using new Azo Schiff compound: electrochemical, gravimetric, adsorption, surface and DFT studies. *J. Mol. Liq.* **2020**, *315*, 113690.
(22) Mubarik, A.; Mahmood, S.; Rasool, N.; Hashmi, M. A.; Ammar, M.; Mutahir, S.; Ali, K. G.; Bilal, M.; Akhtar, M. N.; Ashraf, G. A. Computational Study of Benzothiazole Derivatives for Conformational, Thermodynamic and Spectroscopic Features and Their Potential to Act as Antibacterials. *Crystals* **2022**, *12* (7), 912.
(23) Ahmad, G.; Rasool, N.; Mubarik, A.; Zahoor, A. F.; Hashmi, M. A.; Zubair, M.; Bilal, M.; Hussien, M.; Akhtar, M. S.; Haider, S. Facile Synthesis of 5-Aryl-N-(pyrazin-2-yl) thiophene-2-carboxamides via Suzuki Cross-Coupling Reactions, Their Electronic and Nonlinear Optical Properties through DFT Calculations. *Molecules* **2021**, *26* (23), 7309.
(24) Wu, Y.; Hu, Q.; Liang, H.; Wang, A.; Xu, H.; Wang, L.; He, X. Electrostatic Potential as Solvent Descriptor to Enable Rational Electrolyte Design for Lithium Batteries. *Adv. Energy Mater.* **2023**, *13*, 2300259.
(25) Roy, R. K.; Saha, S. Studies of regioselectivity of large molecular systems using DFT based reactivity descriptors. *Annu. Rep. Prog. Chem., Sect. C: Phys. Chem.* **2010**, *106*, 118−162.
(26) Balakit, A. A.; Makki, S. Q.; Sert, Y.; Ucun, F.; Alshammari, M. B.; Thordarson, P.; El-Hiti, G. A. Synthesis, spectrophotometric and DFT studies of new Triazole Schiff bases as selective naked-eye sensors for acetate anion. *Supramol. Chem.* **2020**, *32* (10), 519−526.
(27) Savjani, J. K.; Mulamkattil, S.; Variya, B.; Patel, S. Molecular docking, synthesis and biological screening of mefenamic acid derivatives as anti-inflammatory agents. *European journal of pharmacology* **2017**, *801*, 28−34.
(28) Sial, N.; Rasool, N.; Rizwan, K.; Altaf, A. A.; Ali, S.; Malik, A.; Zubair, M.; Akhtar, A.; Kausar, S.; Shah, S. A. A. Efficient synthesis of 2, 3-diarylbenzo [b] thiophene molecules through palladium (0) Suzuki−Miyaura cross-coupling reaction and their antithrombolyitc, biofilm inhibition, hemolytic potential and molecular docking studies. *Med. Chem. Res.* **2020**, *29* (8), 1486−1496.

https://doi.org/10.1021/acsomega.3c03183
ACS Omega 2023, 8, 30306−30314